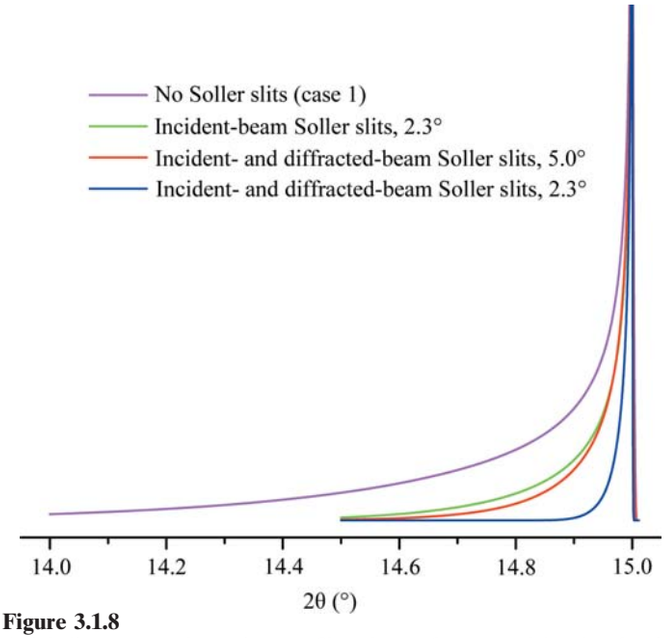

Figure 3.1.8
Axial divergence aberration profiles shown for several levels of axial divergence. Case 1 (of Table 3.1.1) is computed for a source length of 12 mm and a sample and receiving-slit length of 15 mm. The remaining three simulations include are of case 2, where Soller slits limit the axial divergence (R = 217.5 mm).

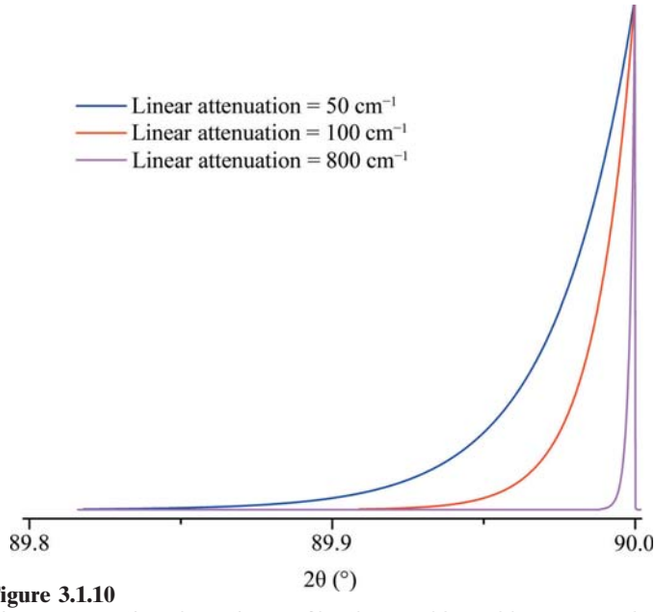

Figure 3.1.10
Linear attenuation aberration profiles that would roughly correspond to SRMs 676a (50 cm^{-1}), 640e and 1976b (100 cm^{-1}), and 660c (800 cm^{-1}) at 90° 2θ, where the transparency effect is at a maximum (R = 217.5 mm).

the path length of the diffracted beam by 10 to 15 cm, reducing axial divergence effects substantially and effectively functioning as a Soller slit. Cheary & Cline (1995) determined that the inclusion of a Soller slit with a post-monochromator did result in a slight improvement in resolution; however, this was at the cost of a threefold reduction in intensity. We do not use Soller slits in the diffracted beam when using a post-monochromator. The 5° primary and secondary Soller slit aberration profile of Fig. 3.1.8 corresponds to an instrument with a primary Soller slit and a graphite post-monochromator. The profiles shown for the two 2.3° Soller-slit configurations actually constitute a fairly high level of collimation given the double-angle definition of the specifications. Fig. 3.1.9 shows the functional dependence of the aberration profile for two 2.3° Soller slits on 2θ. Below approximately 100°, the effect increases with decreasing 2θ. Approximate symmetry is observed at 100°, while asymmetry to high angle increases thereafter. The aberration profile associated with specimen transparency to the X-ray beam is illustrated in Fig. 3.1.10. The figure shows the impact at 90° 2θ where the effect is at its maximum. The observed profile is broadened asymmetrically to low 2θ; the effect drops off in a largely symmetric manner with 2θ on either side of 90°.

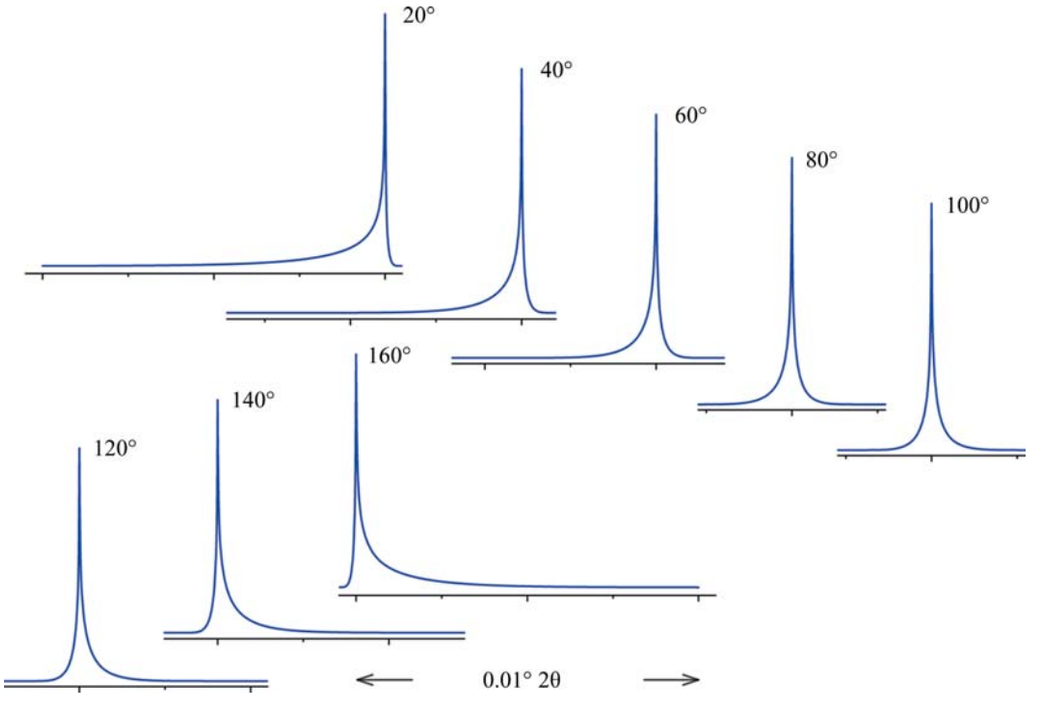

Figure 3.1.9
Axial divergence aberration profiles for primary and secondary Soller slits of 2.3° as a function of 2θ (R = 217.5 mm).

The wavelength profile or emission spectrum with its characterization on an absolute energy scale provides the traceability of the diffraction measurement to the International System of Units (SI) (BIPM, 2006). The currently accepted characterization of the emission spectrum of Cu $K\alpha$ radiation is provided by Hölzer *et al.* (1997) and is shown in Fig. 3.1.11. The spectrum is modelled with four Lorentzian profile shape functions (PSFs): two large ones for the primary $K\alpha_1$ and $K\alpha_2$ profiles, and two smaller ones displaced slightly to lower energy to account for the asymmetry in the observed line shape. The data shown in Fig. 3.1.11 are in energy space and are transformed into 2θ space with the dispersion relation. This is obtained by differentiating